Journal of Alloys and Compounds 735 (2018) 2373–2377

Contents lists available at ScienceDirect

Journal of Alloys and Compounds

journal homepage: http://www.elsevier.com/locate/jalcom

In-situ TEM and XRD analysis of microstructures changes in solution-grown copper silicide nanowires array for field emitters

Chiu-Yen Wang [a, *], Fang-Wei Yuan [b], Yu-Chen Hung [a], Ya-Wen Su [c], Hsing-Yu Tuan [b, **]

[a] Department of Materials Science and Engineering, National Taiwan University of Science and Technology, 43 Sec. 4 Keelung Rd, Taipei 10607, Taiwan
[b] Department of Chemical Engineering, National Tsing Hua University, 101, Section 2, Kuang-Fu Road, Hsinchu 30013, Taiwan
[c] National Nano Device Laboratories, National Applied Research Laboratories, Hsinchu 30078, Taiwan

ARTICLE INFO

Article history:
Received 19 September 2017
Received in revised form
28 November 2017
Accepted 4 December 2017
Available online 6 December 2017

Keywords:
In-situ annealing TEM
Silicide
In-situ annealing XRD
Field emission

ABSTRACT

Pristine polycrystalline copper silicide nanowires were synthesized via facile semi-batch solution reaction on Cu foil at low temperature, 400 °C. Comparing with as-grown products, the annealed (800 °C) Cu_3Si nanowires array exhibits excellent field emission properties, the turn-on field was reduced from 1.16 V/μm to 0.40 V/μm and the field enhancement factor (β) was improved from 1400 to 4637. Field emission properties of the annealed copper silicide nanowires show the performance of field emission could be enhanced through the annealing process. *In-situ* TEM annealing of copper silicide nanowires array was used to investigate the thermal effect on microstructure of copper silicide nanowires. *In-situ* XRD annealing results provide the phase transformation information at varied temperature and show that the transition phase $Cu_{15}Si_4$ existed to assist in growing single crystalline Cu_3Si nanowire. Systemic study can help to realize the solution-phase metal silicide reaction growth mechanism; furthermore, the effect of annealing temperature on nanowires shows the potential towards fabrication of high performance field emission devices.

1. Introduction

Transition metal silicides (MSi_x) are recently applied in many interesting field of science, such as catalysis, high temperature device and microelectronics [1–4]. The lateral dimensions of silicon and metal silicides in integrated circuit (IC) are reduced to sub-micrometer scale. Due to requirement of low electrical resistivity and self-alignment in IC compatible processing, metal silicides can be used as conspicuous interconnects materials. When metal and silicon are mixed together at elevated temperature, the crystalline metal silicide could be epitaxial grown [5–7]. Many kinds of metal silicide nanomaterials were synthesized. Such as titanium silicides ($TiSi_2$ and Ti_5Si_3) [8,9], cobalt silicides (CoSi, and Co_2Si) [10], chromium disilicide ($CrSi_2$) [11], nickel silicides ($NiSi_2$, $Ni_{31}Si_{12}$ and NiSi) [12,13] via metal precursors vapors react with Si substrate under atmosphere pressure; silicide ($GdSi_{1.7}$) [14] via gadolinium vapors react with metal-assisted etching Si nanowires; $Ni_{31}Si_{12}$ and Ti_5Si_4 via using silicon precursors vapors to react with metal foil [15,16] Most of them exhibit high electrical conductivity and excellent electron field emission properties. Furthermore, single crystal metal silicides/germanides nanowire ($NiSi_x$, $CoSi_x$, $NiGe_x$ and $MnGe_x$) [17–20] growth mechanism was studied through metal electrode or metal nanowire reacts with single crystal Si or Ge nanowires under *in situ* annealing TEM. Epitaxial heterostructure of metal silicide (MSi_x)/germanide (MGe_x)-Si/Ge could be prepared through above mentioned method and show excellent transistor properties, since high quality atomic sharp interface between metal silicide/germanide and semiconductor. Phases of metal silicides/germanides are depended on reaction temperature and its oxide capping layer [21,22]. The vapor transport growth of ternary single crystal $CoSi_{1-x}Ge_x$ nanowires could sustain at 950 °C for 30 min without segregation or thermal decomposition through the *in situ* annealing TEM study [23]. It means that the ternary single crystal $CoSi_{1-x}Ge_x$ nanowires have a high thermal stability. However, it still lacks for microstructure variation with annealing temperature study in those metal nanomaterials. In this work, the polycrystalline copper silicide nanowires were synthesized through a solution process at relatively low temperature, 400 °C. After annealing at 800 °C, the polycrystalline copper silicide nanowires array properties of field emitter

* Corresponding author.
** Corresponding author.
E-mail addresses: ChiuYWang@mail.ntust.edu.tw (C.-Y. Wang), hytuan@che.nthu.edu.tw (H.-Y. Tuan).

https://doi.org/10.1016/j.jallcom.2017.12.032
0925-8388/

are remarkable improved. In-situ annealing in TEM and XRD system were used to investigate the microstructure evolution of the polycrystalline copper silicide nanowires. Furthermore, depending on the results of in-situ heating TEM and XRD, grain growth and re-crystalline of nanowires were achieved by annealing and then lead to the annealed Cu_3Si NWs on Cu foil display excellent performance electron field emission.

2. Experimental

Anhydrous benzene and monophenylsilane (MPS, 97%) were purchased from Sigma-Aldrich and Gelest, respectively. Chemicals were stored under argon-filled box and used as received. Copper substrates were purchased from the Taiwan non-ferrous-metal company. The experimental procedure was similar to our previous study [24]. Copper substrates were cleaned with acetone and ethanol and then the reactions were carried out from a semi-batch reaction in a 10 ml titanium (Ti) grade reactor. The substrates were first placed into the Ti reactor under an argon-filled glovebox to make it free for oxygen. The Ti reactor was covered with heating tape and the temperature maintained within ±1.0 °C. The inlet of the Ti reactor was connected to a six-way valve (valco) with a 0.5 ml injection cylinder and the high pressure liquid chromatography (HPLC) pump (Lab Alliance, series 1500) was connected to the six-way valve to deliver the reactant into the reactor. The reactant was prepared in the glovebox with the concentration between 500 mM and 1.0 M. In this reaction process, the reactor was heated to the reaction temperature of 400 °C and was pressurized to 800 psi. Then a 1.0 mL reactant solution was injected into the injection loop at a flow rate of 0.5 mL/min by using the HPLC pump. After reaction, the reactor was submerged in a water bath until it returned to room temperature. Finally, the reacted substrates covered copper silicide nanowires were lift from the reactor for further material characterization. Cu_3Si nanowires were characterized by using scanning electron microscopy (SEM) and transmission electron microscopy (TEM). For high resolution SEM (HRSEM) evaluating, analytical images were including JSM-7000F (JEOL) thermal-type field-emission mode, operated at 15 kV accelerating voltage. For HRTEM analysis, the TEM samples were prepared by drop-casting nanostructures from toluene dilute dispersions onto 200-mesh carbon-coated copper grids (from Electron Microscope Sciences Company). TEM images were acquired using the accelerating voltage of 200 kV and 300 kV on a JEOL JEM-2100F and a JEOL JEM-3000F, respectively. Both of TEM equipment contain an Oxford INCA EDS spectrometer and a high angle annular dark field detector (HAADF). To investigate the annealing effects on Cu_3Si NWs, the samples were lying on a double-tilted heating holder from Gatan 652 for in-situ TEM analysis. The real-time crystallization behavior was video-recorded with a heating rate of 50 °C/min from 25 to 800 °C under the vacuum pressure of 1.0×10^{-6} Torr. X-ray diffraction (XRD) was performed with a Rigaku Ultima IV X-ray diffractometer using Cu Kα radiation (λ = 1.54 Å). The measured samples were put on quartz substrates with a scan rate of 1°/min. For in-situ annealing XRD, samples were laying on heating stage with a heating rate of 10 °C/min and the vacuum kept below 5×10^{-6} Torr to prevent oxidation. The field emission properties of Cu_3Si nanostructures were obtained in a KEITHLY model 237 system with the geometry of the parallel plates with a spacing of 200 μm at a pressure of 3×10^{-6} Torr and the contact area was 0.09 cm^2. The emission current was recorded as the applying voltage increasing with a step of 20 V.

3. Results and discussion

According to our previous study, single crystalline Cu_3Si nanowires could be synthesized at 475 °C and show excellent field emission property [24]. In order to realize the revolution of microstructure within Cu_3Si nanowires that the Cu_3Si nanowires were grown at relatively low temperature, 400 °C. Fig. 1 (a) and (b) are SEM images of the Cu_3Si nanowires grew at 400 °C for 30 s and 1 min, respectively. The shorter growth time, the lower density and the shorter distance of Cu_3Si nanowires were grown on Cu foil. The result was consistent with early study that the Cu_3Si nanomaterials were epitaxial-like grown on Cu grain. Similar results were observed in Ni-Si system that the $Ni_{31}Si_{12}$ nanowires grown on Ni foil and show low turn-on field and high field enhancement factor of field emission [15]. TEM was used to characterize the microstructure of copper silicide products. Fig. 1 (c) and (d) are low and high magnification TEM images that the Cu_3Si nanowires were grown at 400 °C. At the lower growth temperature of 400 °C, the Cu_3Si were not single crystal but comprised of randomly oriented nanocrystals.

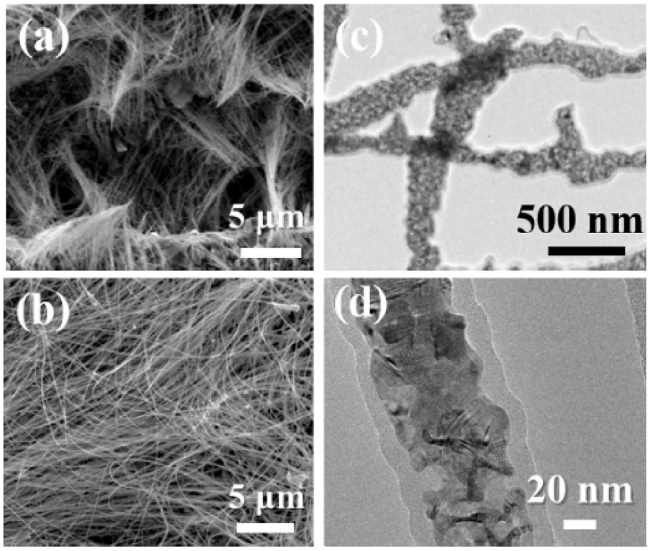

Fig. 1. (a) and (b) are SEM images of copper silicide nanowires that grown for 30 s and 1 min, at 400 °C, respectively. (c) and (d) are zoom-out and zoom-in magnification TEM images of as-grown polycrystalline copper silicide nanowire, respectively.

Cu_3Si nanowires field emission properties were measured, including as-synthesized at 400 °C and as-annealed at 700 and 800 °C. Fig. 2 shows the field emission performance of Cu_3Si nanowires with the current density as a function of the macroscopic electric field. After annealing at 700 and 800 °C, the turn-on field of Cu_3Si nanowires (defined as the electric field to a current density of 100 μA cm^{-2}) were 0.66 and 0.4 V μm^{-1}, respectively Comparing with our previous results, the turn-on field for as-grown sample was estimated to be ~1.2 V μm^{-1}) [24].

The plotted ln (J E^{-2}) versus 1/E, yielding a line and good agreement with the Fowler-Nordheim (F-N) equation given by the following:

$$J = \left(A\beta^2 E^2 / \Phi\right) * \exp\left[-B\Phi^{3/2} / \beta E\right]$$

A and *B* were constants, corresponding to 1.56×10^{-10} ($AeVV^{-2}$) and 6.83×103 ($VeV^{-3/2}\mu m^{-1}$), respectively. J is the current density, Φ is the work function of emitter materials and assuming Φ equals 4.7 eV for Cu_3Si, and β is the field enhancement factor which can be calculated from the slope of the FN plot [24]. After thermal annealing at 700 °C and 800 °C, the β can be determined to be 2810 and 4637, respectively, from the FN plot. These values of annealed samples were much higher than previous studies on different metal

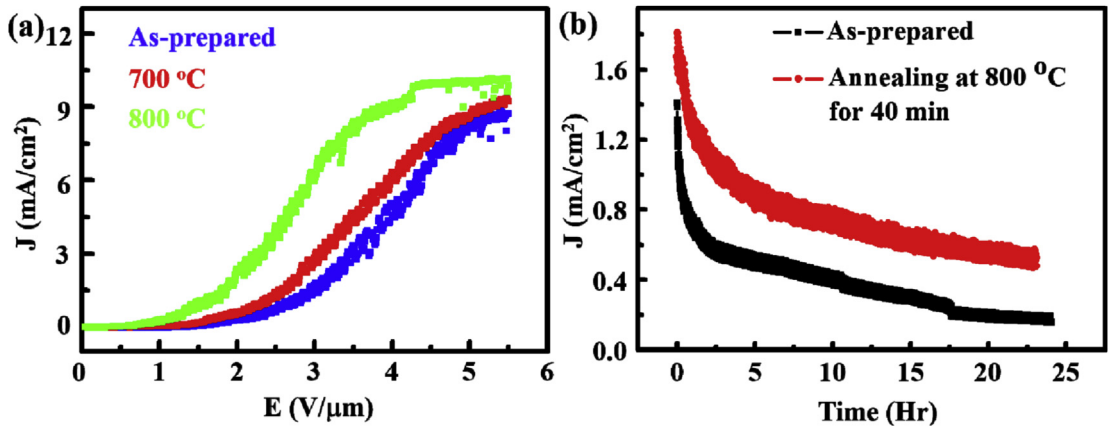

Fig. 2. Electron field emission properties of copper silicide nanowires on Cu substrate. (a) Is the emission current (J, mA/cm^2) to applied electric field (E, V/μm) curves of as-prepared, annealed at 700 °C and 800 °C and (b) is the time dependent current density of as-prepared and annealed at 800 °C for 40 min.

silicide nanostructures. The different field emission performance of Cu_3Si nanowires of before and after thermal annealing may be due to the structure re-crystalline between copper silicide and Cu foil. The distribution of the electric charge in the polycrystalline copper silicide nanostructure may impede the emission of current at the grain boundary. After thermal annealing, larger grain size and small-angle grain boundary will enhance the conductivity and make the electrons more easily to be ejected from the copper silicide nanostructure then result in the excellent field emission performance. This result is the best emitting materials of metal silicide nanostructure reported so far [8–16,24–26]. Comparisons of different silicon-based nanomaterials in terms of turn-on field and field enhancement factor,β, are listed in Table 1. The turn-on field and β in this work of copper silicide nanowires were also considerably much better than or comparable to those of other silicon or silicide nanomaterials.

In order to realize the microstructure evolution of copper silicide nanowires, a two-step thermal annealing process by *in-situ* heating TEM. First, copper silicide nanostructures were synthesized in titanium reactor at low reaction temperature, 400 °C. The copper silicide nanowires were polycrystalline structure, as shown in Fig. 3(a). As the thermal annealing temperature was raised to 500 °C, the re-crystallization happens and the construction of copper silicide nanowires was changed, as shown in Fig. 3 (b). The corresponding diffraction patterns (DP) of as-prepared and after annealed at 700 °C are shown in the inset of Fig. 3 (a) and (b), respectively. Electron diffraction ring pattern in Fig. 3 (a) means the as-prepared copper silicide nanostructure was polycrystalline. After annealing, the diffraction pattern from ring to line means the microstructure transforms from polycrystalline to single crystalline with twin and stacking fault structures. Diffraction patterns in the inset of Fig. 3 (a) and (b) can be used to identify the product is hexagonal η-Cu_3Si unit cell. Fig. 3 (c) and (d) are the bright field and dark field TEM images of the corresponding annealed copper silicide, respectively. The dark field TEM image in Fig. 3 (d) was taken from the diffraction line pattern to confirm the microstructure of annealed copper silicide. The result indicated that the strip line pattern were contributed from twin and stacking fault structures after annealing. Also, as shown in the Fig. 3 (e) was the corresponding atomic resolution TEM image of the twin and stacking fault structures. Since the fast heating rate (50 °C/min) for *in-situ* annealing TEM study, that the details of phase transformation of Cu_3Si NWs were not recorded. Cu_3Si NWs were decomposed as heating to 800 °C under high vacuum 1.0×10^{-6} Torr.

Furthermore, *in-situ* annealing XRD also used to help to realize the influence of annealing impact on Cu_3Si NWs microstructure. The *in-situ* annealing XRD data show that Cu–Si phase strongly depends on the annealing temperature. As shown in Fig. 4, the XRD patterns show that there were two strong peaks at $2\theta = 44.6°$ and 45.0° for the as-prepare samples (grown at 400 °C), those peaks represent the existence of ŋ-phase Cu_3Si crystal structure [24]. Standard XRD patterns of Cu, Cu_3Si $Cu_{15}Si_4$ and CuO are listed to compare with the serial *in situ* annealing XRD data. Once the thermal annealing temperature reach to 500 °C and 700 °C, the strong diffraction peaks at $2\theta = 34.5$, 43.7, 47.8 that contributed from $Cu_{15}Si_4$ (JCPD Card No. 76-1800) [27] were observed and peak intensity at $2\theta = 44.6$ and 45.0 that contributed from Cu_3Si (JCPD Card No. 51-0916) were decreased. These results indicate the copper silicide, $Cu_{15}Si_4$, was formed at higher annealing temperature (500 °C-700 °C). At an annealing temperature as high as 800 °C, the $Cu_{15}Si_4$ peaks at $2\theta = 34.5°$, 43.7°, 47.8° disappear, however, the peak intensity of $2\theta = 44.6°$ increases. That means the ŋ- Cu_3Si was the thermally stable phase and the sample was transformed from $Cu_{15}Si_4$ to ŋ- Cu_3Si and the crystal size might be increased to reduce the grain boundary. It is believed that the excellent field emission property of the annealed copper silicide nanowires is benefited as

Table 1
Comparisons of silicon and metal silicide nanomaterials in terms of turn-on field and field enhancement factor.

Nanowires	Turn-on field (V/μm)	Enhancement factor (β)	Ref.
$TiSi_2$	8.0	501	8
Ti_5Si_3	5.4	816	9
CoSi	1.42	1000	10
$CrSi_2$	3.6	1960	11
$NiSi_2$	7.6	630	12
NiSi	3.0	2200	13
$GdSi_{1.7}$	2.1	1222	14
$Ni_{31}Si_{12}$	1.0	3190	15
Ti_5Si_4	1.47	1350	16
Cu_3Si grown at 470 °C without annealed	1.16	1499	24
Si	5.3	1965	25
$TaSi_2$	4.0	1800	26
Cu_3Si grown at 400 °C without annealed	1.20	1400	This work
Cu_3Si grown at 400 °C annealed at 700 °C	0.66	2810	This work
Cu_3Si grown at 400 °C annealed at 800 °C	0.40	4637	This work

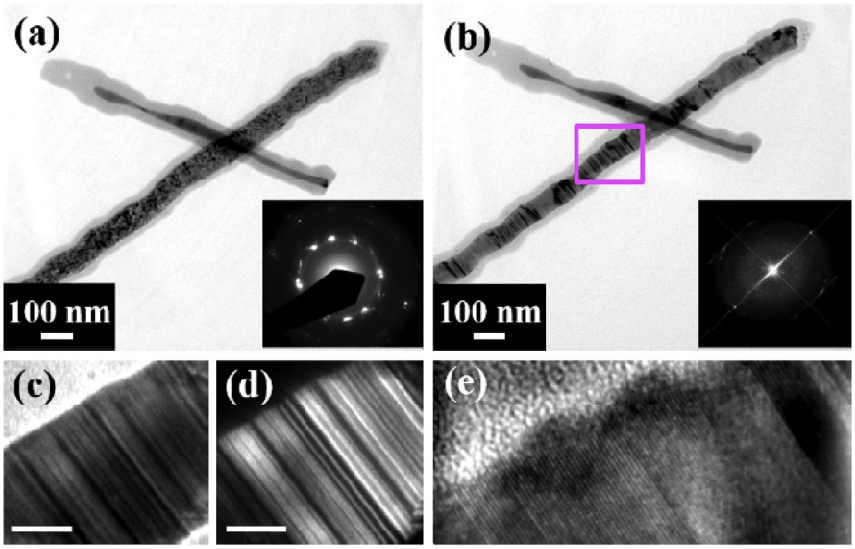

Fig. 3. *In-situ* annealing TEM images of (a) an as-prepared copper silicide nanowire that grown at 400 °C and (b) is after annealing process (from 30 °C to 700 °C then cooling to 30 °C). The corresponding selected area electron diffraction of (a) and (b) are shown in the inset. (c) Is the corresponding selected area high magnification bright field TEM image. (d) Is the dark field and (e) is HRTEM images of the selected copper silicide nanowire. The scale bars in (c) and (d) are 20 nm.

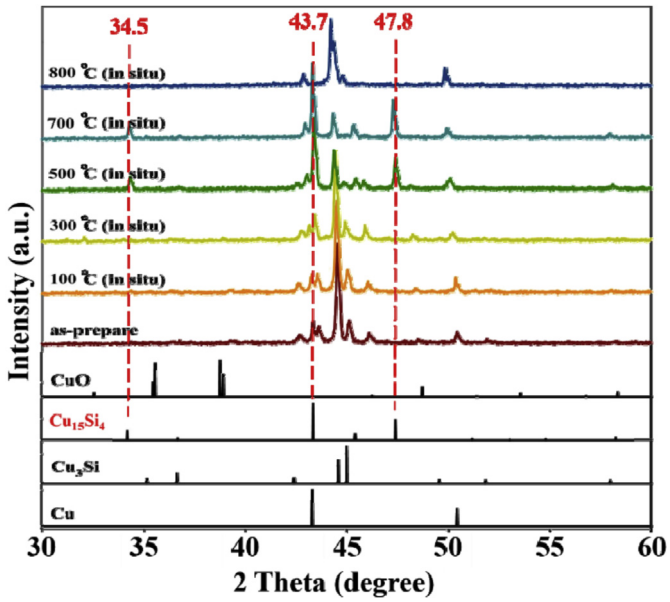

Fig. 4. *In-situ* annealing XRD results of copper silicide nanowires on Cu foil substrate, including as-prepared that grown at 400 °C, 100 °C, 300 °C, 500 °C, 700 °C and 800 °C. Standard XRD patterns of Cu, Cu_3Si $Cu_{15}Si_4$ and CuO are listed to compare with the serial *in-situ* annealing XRD data.

high annealing temperature more than 500 °C to make the composition changing. The results of *in situ* annealing XRD were consisted with *in situ* annealing TEM study and help to understand the phase transformation behavior during polycrystalline copper silicide nanowires annealing.

4. Conclusions

Copper silicide nanowires were synthesized by thermal decomposition of MPS in the presence of a low-cost, commercially available material, Cu seed substrate at 400 °C in supercritical benzene solution. The low turn-on field and high field enhancement factor of Cu_3Si nanowires were achieved through annealing the low temperature grown polycrystalline Cu_3Si nanowires. *In situ* annealing TEM and XRD analyses were used to characterize the microstructure and phase transformation of the annealed polycrystalline copper silicide nanowires.

Conflict of interest

There are no conflicts to declare.

Authors' contributions

Chiu-Yen Wang, Fang-Wei Yuan, Yu-Chen Hung and Ya-Wen Su performed the experiments, analyzed the results, and wrote the manuscript. Chiu-Yen Wang and Fang-Wei Yuan participated in the sample fabrication and characterizations. Chiu-Yen Wang and Hsing-Yu Tuan contributed to the data interpretation and supervised the research. All authors read and approved the final version of the manuscript.

Acknowledgements

Chiu-Yen Wang and H.-Y. T acknowledge the financial support by the Ministry of Science and Technology through the grants of MOST 106-2221-E-011-059, MOST 103-2218-E-011-007-MY3 and MOST 103-2221-E-007-089-MY3.

References

[1] S.J. Jung, T. Lutz, A.P. Bell, E.K. McCarthy, J.J. Boland, Free-standing, single-crystal Cu_3Si nanowires, Cryst. Growth Des. 12 (2012) 3076–3081.
[2] A.L. Schmitt, J.M. Higgins, J.R. Szczech, S. Jin, Synthesis and applications of metal silicide nanowires, J. Mater. Chem. 20 (2010) 223–235.
[3] B. Cao, T.R. Yang, G.P. Li, S. Cho, H. Kim, Atomic diffusion and interface reaction of Cu/Si (111) films prepared by ionized cluster beam deposition, Vacuum 89 (2013) 105–108.
[4] S.M. Yoon, H.J. Song, H.C. Choi, p-Type semiconducting GeSe combs by a vaporization-condensation-recrystallization (VCR) process, Adv. Mater. 22 (2010) 2164–2167.
[5] A.L. Schmitt, S. Jin, Selective patterned growth of silicide nanowires without the use of metal catalysts, Chem. Mater. 19 (2007) 126–128.
[6] H.K. Lin, H.A. Cheng, C.Y. Lee, H.T. Chiu, Chemical vapor deposition of TiSi nanowires on C54 $TiSi_2$ thin film: an amorphous titanium silicide interlayer

assisted nanowire growth, Chem. Mater. 21 (2009) 5388–5396.
[7] J.R. Szczech, S. Jin, Epitaxially-hyperbranched FeSi nanowires exhibiting merohedral twinning, J. Mater. Chem. 20 (2010) 1375–1382.
[8] H.C. Hsu, W.W. Wu, H.F. Hsu, L.J. Chen, Growth of high-density titanium silicide nanowires in a single direction on a silicon surface, Nano Lett. 7 (2007) 885–889.
[9] H.K. Lin, Y.F. Tzeng, C.H. Wang, N.H. Tai, I.N. Lin, C.Y. Lee, H.T. Chiu, Ti_5Si_3 nanowire and its field emission property, Chem. Mater. 20 (2008) 2429–2431.
[10] C.I. Tsai, P.H. Yeh, C.Y. Wang, H.W. Wu, U.S. Chen, M.Y. Lu, W.W. Wu, L.J. Chen, Z.L. Wang, Cobalt silicide nanostructures: synthesis, electron transport, and field emission properties, Cryst. Growth Des. 9 (2009) 4514–4518.
[11] Y.L. Zhang, Q. Wu, W.J. Qian, N. Liu, X.T. Qin, L.S. Yu, X.Z. Wang, Z. Hu, Morphology-controlled growth of chromium silicide nanostructures and their field emission properties, CrystEngComm 14 (2012) 1659–1664.
[12] C.Y. Lee, M.P. Lu, K.F. Liao, W.F. Lee, C.T. Huang, S.Y. Chen, L.J. Chen, Free-standing single-crystal $NiSi_2$ nanowires with excellent electrical transport and field emission properties, J. Phys. Chem. C 113 (2009) 2286–2289.
[13] C.J. Kim, K. Kang, Y.S. Woo, K.G. Ryu, H. Moon, J.M. Kim, D.S. Zang, M.H. Jo, Spontaneous chemical vapor growth of NiSi nanowires and their metallic properties, Adv. Mater. 19 (2007) 3637.
[14] L.W. Chu, S.W. Hung, C.Y. Wang, Y.H. Chen, J.S. Tang, K.L. Wang, L.J. Chen, Field emission and magnetic properties of free-standing Gd silicide nanowires prepared by reacting ultrahigh vacuum deposited Gd films with well-aligned Si nanowires, J. Electrochem. Soc. 158 (2011) K64–K68.
[15] C.Y. Lee, M.P. Lu, K.F. Liao, W.W. Wu, L.J. Chen, Vertically well-aligned epitaxial $Ni_{31}Si_{12}$ nanowire arrays with excellent field emission properties, Appl. Phys. Lett. 93 (2008), 113109.
[16] C.M. Chang, Y.C. Chang, C.Y. Lee, P.H. Yeh, W.F. Lee, L.J. Chen, Ti_5Si_4 nanobats with excellent field emission properties, J. Phys. Chem. C 113 (2009) 9153–9156.
[17] K.C. Lu, W.W. Wu, H.W. Wu, C.M. Tanner, J.P. Chang, L.J. Chen, K.N. Tu, In situ control of atomic-scale Si layer with huge strain in the nanoheterostructure NiSi/Si/NiSi through point contact reaction, Nano Lett. 7 (2007) 2389–2394.
[18] Y.C. Chou, W.W. Wu, S.L. Cheng, B.Y. Yoo, N. Myung, L.J. Chen, K.N. Tu, In-situ TEM observation of repeating events of nucleation in epitaxial growth of nano $CoSi_2$ in nanowires of Si, Nano Lett. 8 (2008) 2194–2199.
[19] J. Tang, C.Y. Wang, F. Xiu, A.J. Hong, S.Y. Chen, M. Wang, C. Zeng, H.J. Yang, H.Y. Tuan, C.J. Tsai, L.J. Chen, K.L. Wang, Single-crystalline Ni_2Ge/Ge/Ni2Ge nanowire heterostructure transistors, Nanotechnology 21 (2010), 505704.
[20] J. Tang, C.Y. Wang, L.T. Chang, Y. Fan, T. Nie, M. Chan, W. Jiang, Y.T. Chen, H.J. Yang, H.Y. Tuan, L.J. Chen, K.L. Wang, Electrical spin injection and detection in Mn_5Ge_3/Ge/Mn_5Ge_3 nanowire transistors, Nano Lett. 13 (2013) 4036–4043.
[21] Y. Chen, Y.C. Lin, X. Zhong, H.C. Cheng, X. Duan, Y. Huang, Kinetic manipulation of silicide phase formation in Si nanowire templates, Nano Lett. 13 (2013) 3703–3708.
[22] J. Tang, C.Y. Wang, F. Xiu, M. Lang, L.W. Chu, C.J. Tsai, Y.L. Chueh, L.J. Chen, K.L. Wang, Oxide-confined formation of germanium nanowire heterostructures for high-performance transistors, ACS Nano 5 (2011) 6008–6015.
[23] C.I. Tsai, C.Y. Wang, J. Tang, M.H. Hung, K.L. Wang, L.J. Chen, Electrical properties and magnetic response of cobalt germanosilicide nanowires, ACS Nano 5 (2011) 9552–9558.
[24] F.W. Yuan, C.Y. Wang, G.A. Li, S.H. Chang, L.W. Chu, L.J. Chen, H.Y. Tuan, Solution-phase synthesis of single-crystal Cu_3Si nanowire arrays on diverse substrates with dual functions as high-performance field emitters and efficient anti-reflective layers, Nanoscale 5 (2013) 9875–9881.
[25] Y.L. Chueh, L.J. Chou, S.L. Cheng, J.H. He, W.W. Wu, L.J. Chen, Synthesis of taperlike Si nanowires with strong field emission, Appl. Phys. Lett. 86 (2005), 133112.
[26] Y.L. Chueh, M.T. Ko, L.J. Chou, L.J. Chen, C.S. Wu, C.D. Chen, $TaSi_2$ nanowires: a potential field emitter and interconnect, Nano Lett. 6 (2006) 1637–1644.
[27] H. Geaney, C. Dickinson, C. O'Dwyer, E. Mullane, A. Singh, K.M. Ryan, Growth of Crystalline Copper silicide nanowires in high yield within a high boiling point solvent system, Chem. Mater. 24 (2012) 4319–4325.